

Turbulence and Mixing in the Intracluster Medium

P. Sharma*, B. D. G. Chandran[†], E. Quataert* and I. J. Parrish*

* *Theoretical Astrophysics Center and Astronomy Department, University of California, Berkeley, CA 94720, USA*

[†] *Space Science Center and Department of Physics, University of New Hampshire, Durham, NH 03824, USA*

Abstract. The intracluster medium (ICM) is stably stratified in the hydrodynamic sense with the entropy s increasing outwards. However, thermal conduction along magnetic field lines fundamentally changes the stability of the ICM, leading to the “heat-flux buoyancy instability” when $dT/dr > 0$ and the “magnetothermal instability” when $dT/dr < 0$. The ICM is thus buoyantly unstable regardless of the signs of dT/dr and ds/dr . On the other hand, these temperature-gradient-driven instabilities saturate by reorienting the magnetic field (perpendicular to $\hat{\mathbf{r}}$ when $dT/dr > 0$ and parallel to $\hat{\mathbf{r}}$ when $dT/dr < 0$), without generating sustained convection. We show that after an anisotropically conducting plasma reaches this nonlinearly stable magnetic configuration, it experiences a buoyant restoring force that resists further distortions of the magnetic field. This restoring force is analogous to the buoyant restoring force experienced by a stably stratified adiabatic plasma. We argue that in order for a driving mechanism (e.g. galaxy motions or cosmic-ray buoyancy) to overcome this restoring force and generate turbulence in the ICM, the strength of the driving must exceed a threshold, corresponding to turbulent velocities $\gtrsim 10 - 100$ km/s. For weaker driving, the ICM remains in its nonlinearly stable magnetic configuration, and turbulent mixing is effectively absent. We discuss the implications of these findings for the turbulent diffusion of metals and heat in the ICM.

Keywords: convection; cooling-flows; clusters

PACS: 98.65.Cw, 98.65.Hb

INTRODUCTION

One of the important developments in the study of galaxy clusters during the last decade has been the discovery that very little gas cools to low temperatures in cluster cores [14, 10]. Strong cooling flows are expected in the absence of non-adiabatic heating of the ICM [6]. The lack of cooler gas suggests that heating, most likely due to feedback from the central Active Galactic Nucleus (AGN), roughly balances cooling. Although the plasma does not cool catastrophically, observational signatures of cooling ($H\alpha$ filaments) and feedback (radio bubbles) are seen in many clusters [4]. Energetically, there are many heat sources that can balance cooling in cluster cores: thermal conduction from larger radii [2]; heating by jets and bubbles [3]; heating by cosmic rays [5, 7]; etc. However, the challenge is to identify an *isotropic* heating mechanism that can balance cooling over many cooling timescales without violating the observational constraints.

The focus of this paper is on the transport and mixing properties of the ICM, and not on a particular ICM heating mechanism. Important advances in understanding the convective stability of the ICM have been made over the past few years. In particular, it has been realized that the ICM is buoyantly unstable in the presence of thermal

conduction along magnetic field lines, regardless of the signs of the temperature and entropy gradients, dT/dr and ds/dr . In cluster cores, where $dT/dr > 0$, the ICM is unstable to the “heat-flux-driven buoyancy instability” (HBI) [16], and at larger radii where $dT/dr < 0$ the plasma is unstable to the “magnetothermal instability” (MTI) [1]. The action of these instabilities is to reorient the magnetic field, so that field lines become perpendicular to ∇T when $dT/dr > 0$ and parallel to ∇T when $dT/dr < 0$ ([11, 12, 17]). In cluster cores, the reorientation of the magnetic field effectively shuts off thermal conduction, resulting in a catastrophic cooling flow [13]. Our goal in this paper is to evaluate the broader effect of thermal conduction on the mixing and transport properties of the ICM; in particular, to determine how effectively heating concentrated in some specific volume due to external driving (e.g., by AGN jets, galaxy wakes) can be redistributed throughout the ICM. To address this we focus on convective transport driven by cosmic rays, and show that the turbulence is spread out (both in r and in θ and ϕ) more effectively with thermal conduction than without it. We interpret this in terms of the Richardson number, the ratio of the buoyancy and turbulent forces. The governing equations, numerical simulations, and the initial set-up have been discussed in detail in [18] and have not been repeated here.

RESULTS

The numerical simulations that we discuss are based on the standard MHD equations but with thermal conduction (both isotropic and anisotropic [i.e., along magnetic field lines]). In addition, cosmic rays are evolved as a relativistic fluid with the same bulk velocity as that of the thermal plasma, which couples to the plasma via its pressure in the momentum equation. Diffusion of cosmic rays along magnetic field lines is included; however, cosmic rays, within a reasonable range of diffusion coefficients, are effectively adiabatic for the scales of interest.

In [18] we studied in detail the convective instability driven by the gradient in the cosmic-ray ‘entropy’ (defined as $p_{\text{cr}}/\rho^{4/3}$, where p_{cr} is the cosmic-ray pressure and ρ is the plasma density), which arises when the cosmic-ray pressure is a significant fraction of the thermal pressure and the cosmic-ray ‘entropy’ decreases outwards. We found that cosmic-ray-driven convection stirs the ICM, both in radius and angle, when the cosmic-ray pressure is sufficiently large.

Here, we focus on the general mixing properties of the ICM; cosmic-ray convection is only one of the plausible mechanisms for generating turbulence (others being, AGN jets, galactic wakes, etc.). We inject cosmic rays only within a narrow range of angles ($\theta < 30^\circ$) about the poles; the cosmic-ray pressure is built up by a steep (such that the cosmic-ray ‘entropy’ decreases outwards) cosmic-ray source term (see [18] for details). We compare three simulations with initial temperature and density profiles similar to those observed in typical cluster cores (the simulation parameters are the same as in runs CR30 and CR30-ad of [18], except that these are axisymmetric runs): (1) plasma with thermal conduction (Spitzer value) along magnetic field lines; (2) plasma with isotropic (Spitzer value) thermal conduction; and (3) adiabatic plasma with no thermal conduction. Plasma cooling is not included in these runs, as the focus is on the effect of thermal conduction on plasma mixing.

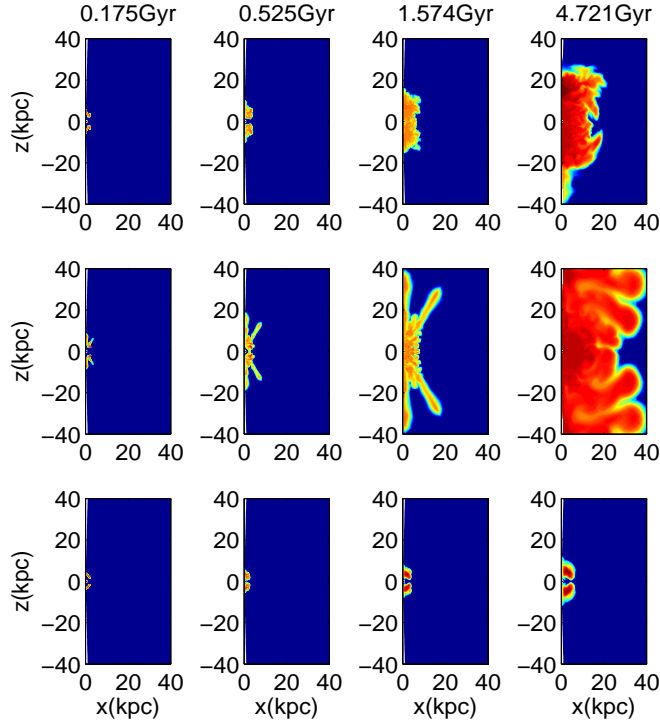


FIGURE 1. Metallicity (logarithmic) profiles (scaled by its maximum value in the particular plot) at different times for runs with anisotropic thermal conduction (top row), isotropic thermal conduction (middle row), and adiabatic plasma (bottom row). A passive scalar initialized within inner four grid points (<1.25 kpc) is used as a proxy for metallicity. While mixing driven by cosmic-ray convection is most efficient with isotropic thermal conduction, it is least effective for an adiabatic plasma. See the text for details.

Figure (1) shows metallicity profiles at different times for runs with anisotropic conduction (top row), isotropic conduction (middle row), and no thermal conduction (i.e., adiabatic plasma; bottom row). Mixing is efficient with thermal conduction, and a large volume of plasma (even at the equator, although the cosmic-ray source only operates near the poles) is mixed by cosmic-ray-driven convection. This figure is analogous to Figure (11) in [18], but is based on two-dimensional (axisymmetric) simulations and includes the isotropic conduction case. Here, instead of the ratio of cosmic-ray and plasma pressures (as in Fig. [11] of [18]), we show metallicity. Like metals, cosmic rays (and possibly heat from other sources of ICM heating) are also more efficiently spread out (in both r and θ) with conduction than without it. It is curious that mixing with isotropic thermal conduction is even more widespread than with anisotropic thermal conduction. These differences are explained in detail in the next section.

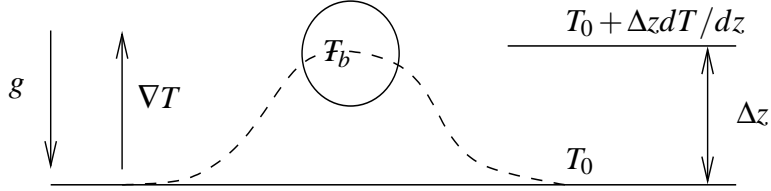


FIGURE 2. Cartoon for the blob displaced from the initial stable/saturated HBI state (with horizontal field lines shown by the solid line) for $dT/dz > 0$ (\hat{z} is taken along the radial direction). The blob is displaced vertically by Δz ; the dashed line shows the perturbed weak magnetic field. In the fast-conduction limit the blob temperature is the same as the temperature of the initial field line; i.e., $T_b = T_0$. In the Boussinesq limit the blob pressure equals the background pressure at Δz ($= p_0 + \Delta z dp/dz$). The buoyancy force on the blob is $(\rho_b - \rho_0 - \Delta z d\rho/dz)g$, corresponding to the density difference of the blob relative to its surroundings. Expressing the density in terms of the temperature and pressure, the buoyancy force reduces to $\rho g \Delta z d \ln T / dz$ in the direction of gravity, i.e., a restoring force.

EFFECT OF TURBULENT FORCING

There is a fundamental difference between convection in anisotropically conducting plasmas and the more well-known Schwarzschild convection that arises in adiabatic plasmas. While the energy in Schwarzschild convection is mainly transported by fluid motions, it is transported by thermal conduction in anisotropically conducting plasmas (even when $dT/dz > 0$ [\hat{z} is along the radial direction], in which case field lines in the saturated state are aligned almost perpendicular to the temperature gradient). In addition, the turbulent velocities in the saturated state in buoyantly unstable, anisotropically conducting plasmas are very small (e.g., table 1 in [12] shows that the rms Mach numbers are $\lesssim 10^{-3}$ even when the vertical temperature gradient is large and the temperatures are fixed at the vertical boundaries; also [17]). In contrast, in Schwarzschild convection the turbulent velocities can be much larger, and turbulent velocities are larger for larger entropy gradients across the box.

From the above discussion (that the velocities are negligible with free convection [MTI/HBI] in anisotropically conducting plasma) we can consider a static saturated state for these instabilities with anisotropic thermal conduction. Figure (2) considers a blob being perturbed from its HBI saturated state ($dT/dz > 0$ in the background plasma) with horizontal field lines. The perturbed blob is at the same temperature as the original field line (T_0). In the Boussinesq limit the blob is at the same pressure as the background pressure at the perturbed position. The buoyancy force on the blob is a restoring force ($\rho g \Delta z d \ln T / dz$), bringing the blob back to its original position (see the figure caption). In this sense the HBI saturated state with horizontal field lines (and negligible velocities) is the stable state of an anisotropically conducting plasma with $dT/dz > 0$. Analogous considerations for the MTI saturated state with vertical field lines when $dT/dz < 0$, show that a vertically displaced blob experiences a similar restoring force ($\rho g \Delta z |d \ln T / dz|$).¹

¹ The vertical field lines are not isothermal, but the conductive heat flux \mathbf{Q} in the displaced blob satisfies $\nabla \cdot \mathbf{Q} = 0$; see [16] who invoke a similar argument for the destabilization of vertical field lines with $dT/dz > 0$.

Thus, it is clear that a horizontally (vertically) aligned magnetic field with negligible velocity is the saturated or nonlinearly *stable* state for the HBI (MTI). In other words, horizontal field lines (when $dT/dz > 0$) and vertical field lines (when $dT/dz < 0$) are the stable configurations of the system, and the HBI and MTI are buoyancy instabilities that bring the system to this stable configuration (thus in this sense an anisotropically conducting plasma is analogous to a stably stratified adiabatic plasma, in that a perturbed blob experiences a restoring force). Only tiny velocities (ignoring magnetic tension and assuming that the conduction time is shorter than the Brunt-Väisälä time) bring the initially unstable system to its stable state (with reoriented field lines); after that there is no turbulent driving and the velocities decay with time ([12] & [11]). This is entirely different from convection in adiabatic plasmas where turbulent velocities are driven as long as the entropy gradients are sustained by the boundary conditions at the upper and lower boundaries of the convective region.

Although the buoyant restoring force in the HBI/MTI-saturated state resists distortions of the magnetic field, if an anisotropically conducting plasma is stirred sufficiently strongly to drive it away from its stable magnetic configuration and tangle up the magnetic field, then the buoyancy forces in this tangled-magnetic-field state could in principle add to (or subtract from) the turbulent driving force. This effect, however, is not expected to change the turbulent velocities by more than a factor of order unity.

To understand why mixing is more effective with isotropic conduction than with anisotropic conduction in Figure (1), consider a blob perturbed from its mean position by Δz ; now, since the conductivity is large, the displaced blob has almost the same temperature as the background plasma at the same height. In the Boussinesq approximation the blob's internal pressure is the same as the external pressure at the same height. When the blob has the same pressure and almost the same temperature as its surroundings, there is almost no density difference, and hence the buoyancy force is nearly zero. Because of this neutral buoyant response it is much easier for a turbulence-driving mechanism such as cosmic-ray buoyancy or galaxy motions to disperse a plasma with isotropic conduction than an adiabatic or anisotropically conducting plasma.

The ability of driven turbulence to overcome the stabilizing effect of anisotropic conduction (i.e., the tendency to pull back to horizontal [vertical] field lines with $dT/dz > 0$ [< 0]) can be quantified in terms of the Richardson number, a quantity often used in studies of forced turbulence in stably stratified systems [19]. The Richardson number (Ri) is the ratio of the restoring buoyant force to the random convective ($\rho \mathbf{u} \cdot \nabla \mathbf{u}$) force, which can be thought of as driving a random walk of the displaced blob. The effect of the stabilizing influence (either for stably stratified adiabatic plasma or for anisotropically conducting plasma) can be overcome if the turbulent forcing rate is larger than the rate of the stable buoyant response (i.e., the Brunt-Väisälä frequency for a stably stratified plasma, or $[g|d \ln T/dz|]^{1/2}$ for an anisotropically conducting plasma). This condition for effective turbulent mixing can be recast into the form $Ri < Ri_c$, where Ri_c is the critical Richardson number below which the random turbulent forces can overcome the effects of the stable buoyant response. ($Ri_c \approx 1/4$ is found in hydrodynamic studies of stably stratified systems [19].) The precise value of Ri_c for anisotropically conducting plasmas, and its dependence on the initial field geometry, will be determined in future with numerical simulations.

DISCUSSION

On cluster core scales, where the thermal conduction time is shorter than the Brunt-Väisälä timescale, a hypothetical, isotropically conducting plasma would have $Ri \approx 0$ (a neutral buoyant response to external forcing; see previous section), and hence the efficient mixing seen in Figure (1). On the other hand, anisotropically conducting intracluster plasma naturally evolves to its stable saturated state (i.e., magnetic field lines perpendicular to ∇T when $dT/dr > 0$), in which the gentle positive temperature gradient (as compared to a steep entropy gradient) results in a small stabilizing buoyant force. Defining $Ri \equiv gr(d\ln T/d\ln r)/u^2$ for the anisotropically conducting core, where g is the gravitational acceleration, u is the typical forcing velocity and r is the radius (r is assumed to be the only scale in the problem but if the most effective turbulent driving is at a different scale this definition should be rescaled accordingly); for adiabatic plasma the temperature gradient is replaced by the entropy gradient. Thus, the Richardson number evaluated for typical cluster conditions is

$$Ri \approx 3g_{-8}r_{10} \frac{d\ln T/d\ln r}{u_{100}^2}, \quad (1)$$

where g_{-8} is the gravitational acceleration in the units of $10^{-8} \text{ cm}^2\text{s}^{-1}$, r_{10} is the scale height (taken roughly to be the radius) in the units of 10 kpc, u_{100} is the shear velocity in the units of 100 km s^{-1} . A typical logarithmic temperature gradient in cluster cores is $d\ln T/d\ln r \approx 0.15$, and the typical logarithmic entropy gradient is $d\ln s/d\ln r \approx 0.6$ (e.g., [15]). Thus, from the requirement that $Ri < Ri_c$ (since only a single spatial scale is used in defining Ri in Eq. [1], $Ri_c \approx 1/4$ is only a rough estimate for the critical value) for efficient turbulent mixing, turbulent velocities $\sim 100 \text{ km s}^{-1}$ are sufficient for efficient mixing in the cluster core and for overcoming the restoring force experienced by a plasma in the HBI-saturated state (see Fig. [5] in [18]; similar velocities are seen in vigorously stirred regions in the top panel of Fig. [1]; although turbulent velocities in [18] are driven by cosmic-ray convection the above criterion for turbulent mixing applies more generally). Because $ds/d\ln r \simeq 4|d\ln T/dr|$, a four-times-larger turbulent energy would be required to induce forced mixing in a hypothetical adiabatic cluster core. Since isotropically conducting plasma has a neutral buoyant response, it can be effectively mixed by much smaller turbulent velocities. Consistent with the above, the turbulent velocities (in the well-mixed regions) in the isotropically conducting case are the smallest, followed by the anisotropically conducting case, and by the adiabatic case.

Although these considerations provide a qualitative understanding of mixing and turbulence in the ICM, realistic numerical simulations, including cooling, are required for understanding the role of forced turbulence (e.g., by cosmic rays, shear instabilities at the jet boundary, etc.) in heating the ICM and spreading the heat isotropically. Although we have focused on cluster cores with $dT/dr > 0$, similar considerations for mixing and turbulence apply at larger radii where $dT/dr < 0$. The ICM plasma can be driven turbulent by the infalling dark-matter halos and galaxy wakes if large turbulent velocities (10-100 km/s) are generated. The stability of the anisotropic plasma in its saturated state (i.e., horizontal field lines with $dT/dr > 0$ and vertical field lines with $dT/dr < 0$) has important implications for the effective thermal conductivity of the ICM. It is sometimes

argued (e.g., [9]) that the ICM should be turbulent and the effective thermal conductivity should be a fraction ($\approx 1/3$) of the Spitzer value. In light of the arguments presented in this paper, isotropic turbulence (leading to $\approx 1/3$ Spitzer conduction) can only be driven if the magnitude of turbulent driving is reasonably large ($\sim 10\text{-}100 \text{ km s}^{-1}$); for a lower magnitude of turbulent stirring the ICM plasma will relax to its stable state with anisotropic thermal conduction (i.e., horizontal field lines in the ICM core where $dT/dr > 0$ and vertical field lines in outer regions where $dT/dr < 0$). Thus, in the absence of vigorous turbulent stirring, the effective conductivity (normalized to the Spitzer value) is $\lesssim 0.1$ (e.g., [12]) in the ICM core and ~ 1 in the outer regions. Such a drastic modification of the thermal conductivity has implications for the role of thermal conduction in solving the cooling flow problem (e.g., see [13]).

The stability of a stably stratified adiabatic plasma and an anisotropically conductive plasma is analogous to the hydrodynamic stability of Keplerian flows (e.g., [8]). In both cases there is a restoring force (epicyclic stabilization for Keplerian flows and buoyant stabilization in anisotropically conducting stratified plasmas) that brings the perturbed fluid element back to its original location. The focus in hydrodynamic disks has been on the nonlinear stability of Keplerian flows and not so much on the forced driving of turbulence and transport, but it is likely that a Richardson-like criterion, that the shearing rate due to the sustained nonlinear velocities be larger than the epicyclic frequency, holds for these linearly stable hydrodynamic shear flows.

In addition to the effect of thermal conduction on free convection (via HBI, MTI), its effect on forced convection (e.g., turbulent forcing by jets, cosmic rays, etc.) is also crucially important, especially in cluster cores, where strong kinetic feedback mechanisms are expected to operate. In most of the discussion, the effect of magnetic tension is ignored and the conduction time is assumed to be much shorter than buoyancy timescale. For more details on the numerical setup, initial and boundary conditions, etc. refer to [18].

ACKNOWLEDGMENTS

Support for this work was provided by NASA through Chandra Postdoctoral Fellowship grant numbers PF8-90054 (to PS, EQ) and PF7-80049 (to IJP, EQ) awarded by the Chandra X-ray Center, which is operated by the Smithsonian Astrophysical Observatory for NASA under contract NAS8-03060. This research was supported in part by the National Science Foundation through TeraGrid resources provided by NCSA and Purdue University.

REFERENCES

1. S. Balbus 2000, ApJ, 534, 420
2. E. Bertschinger & A. Meiksin 1986, ApJ, 306, L1
3. J. Binney & G. Tabor 1995, MNRAS, 276, 663
4. K. W. Cavagnolo, M. Donahue, G. M. Voit, & M. Sun 2008, ApJ, 683, L107
5. B. D. G. Chandran & Y. Rasera 2007, ApJ, 671, 1413
6. A. C. Fabian 1994, ARA&A, 32, 277

7. F. Guo & S. P. Oh 2008, MNRAS, 384, 251
8. J. F. Hawley, S. A. Balbus, & W. F. Winters 1999, 518, 394
9. R. Narayan & M. V. Medvedev 2001, ApJ, 562, L129
10. C. P. O'Dea, et al. 2008, ApJ, 685, 1035
11. I. J. Parrish & J. M. Stone 2007, ApJ, 664, 135
12. I. J. Parrish & E. Quataert 2008, ApJ, 677, L9
13. I. J. Parrish, E. Quataert, & P. Sharma 2009, ApJ, 703, 96
14. J. R. Peterson, et al. 2003, ApJ, 590, 207
15. R. Piffaretti, Ph. Jetzer, J. S. Kaastra, & T. Tamura 2005, A&A, 433, 101
16. E. Quataert 2008, ApJ, 673, 758
17. P. Sharma, E. Quataert, & J. M. Stone 2008, MNRAS, 389, 1815
18. P. Sharma, B. D. G. Chandran, E. Quataert, & I. Parrish 2009, ApJ, 699, 348
19. J. S. Turner in "Buoyancy Effects in Fluids," Cambridge Univ. Press, 1973

